NASA TECHNICAL NOTE

NASA TN D-2990

IMAGE DISSECTOR APERTURE GEOMETRIES AND SCAN PATTERNS FOR USE IN STAR TRACKER SYSTEMS

by Fred H. Shigemoto and Bruce H. Dishman

Ames Research Center

Moffett Field, Calif.

NATIONAL AERONAUTICS AND SPACE ADMINISTRATION • WASHINGTON, D. C. • SEPTEMBER 1965

NASA TN D-2990

IMAGE DISSECTOR APERTURE GEOMETRIES AND SCAN PATTERNS FOR USE IN STAR TRACKER SYSTEMS

By Fred H. Shigemoto and Bruce H. Dishman

Ames Research Center
Moffett Field, Calif.

NATIONAL AERONAUTICS AND SPACE ADMINISTRATION

For sale by the Clearinghouse for Federal Scientific and Technical Information
Springfield, Virginia 22151 – Price $2.00

IMAGE DISSECTOR APERTURE GEOMETRIES AND SCAN PATTERNS FOR USE IN STAR TRACKER SYSTEMS

By Fred H. Shigemoto and Bruce H. Dishman
Ames Research Center

SUMMARY

A study was made of different aperture geometries which could be placed at the electron image plane of an image dissector tube to derive electrical signals of star position relative to the optical axis. In comparison to the conventional image dissector tube with circular aperture and circular scan, it was anticipated that improved signal linearity, reduced cross coupling, and a star presence signal could be achieved and that the major complexity of deriving position information could be included in the reticle geometry rather than in the electronic circuitry.

The aperture geometry in conjunction with the lissajous figure formed by the deflected electron beam is the basis of position detection by means of an image dissector. To avoid the expense and delay of manufacturing a series of modified tubes, a simulation of the internal operation of the image dissector was devised. This simulator was used to test a number of different combinations of aperture and scan pattern. The tests validated the simulation procedure and showed the saw-toothed reticle to be superior to the others tested. An actual tube with a saw-tooth reticle was then manufactured and the improved performance was as expected. Although the size of the linear region is greatly improved there is also an increase in dark current due to the large aperture area. In this study, the aperture geometry was of primary importance for extending the linearity of the output signal; the possibility of using a complicated scan with a very small aperture to obtain the tracker characteristic desired was not considered.

Author

INTRODUCTION

The essential elements of any star tracker system are the optics, modulation technique, and the photodetector. The problem is to derive electrical signals proportional to the displacement of the image relative to the optical axis. These signals can be generated by various methods which can be categorized into two groups: first, those systems which mechanically modulate the incoming light according to its displacement relative to the optical axis, and second, those systems in which the optical image is converted to an electronic image and modulated electronically. The disadvantage of the first type is that the lifetime and reliability of the system are limited by the mechanically moving parts. This disadvantage can be largely overcome with systems of the second type which use image tubes such as the vidicon, the image orthicon, and the image dissector. The primary feature of the image

dissector tube is its ability to electronically deflect the electron image over an aperture leading to the electron multiplication section of the tube.

Various investigators have shown that the image dissector can be used effectively as a detector in star tracking systems. The tube in these systems has the conventional circular aperture. This report is concerned with an investigation of other aperture shapes designed to improve image dissector tube performance in star tracker applications. Specific objectives were to simplify the electronic scan circuitry, and also to obtain a larger linear operating region. In order to carry out the investigation most effectively, an electronic simulator of the internal operation of the image dissector was developed.

IMAGE DISSECTOR AND ITS SIMULATION

An image dissector in a typical operating mode is sketched in figure 1. An optical image on the photocathode is converted to an electron beam which can be deflected and is accelerated to the aperture plane. Electrons passing through the aperture enter the dynode structure of the tube and result in an output signal. Appendix A describes in detail the operation of the tube. Its two primary parameters in generating star image position information are the geometry of the aperture and the lissajous scan pattern. When the scan pattern is superimposed on the aperture, a time sequence of pulses emerges from the tube. The position and duration of each pulse are determined by the sections of the aperture through which the electrons pass. For a given aperture and scan pattern the characteristics of the pulse output are changed by the displacement of the centroid of the scan pattern. Thus, position information of the optical image relative to the optical axis is imparted to the output signal.

For a detector such as the image dissector to function effectively as part of an automatic star tracker system, it should have the following characteristics:

1. Linearity of output signal versus error displacement from null
2. Two-axis output with minimum cross coupling between axes
3. Star presence signal at null
4. Simple electronic circuitry for sweep generation and signal processing

There are several different modifications to the aperture shape and scan pattern of the conventional image dissector that could improve its performance with respect to these characteristics. But to test these modifications actual tubes containing the different apertures would have to be built and evaluated. However, to avoid the delay and expense of manufacturing a series of modified tubes an electro-optical simulation was developed. This simulation permitted various concepts to be evaluated in the laboratory and the best features

selected for the construction of an actual tube. In the simulation the plane of the aperture and the lissajous figure formed by the deflected electron image were represented accurately (fig. 2). The point at which the electron beam is incident on the image plane is represented by a spot on the screen of an oscilloscope. Various lissajous figures can then be formed by deflection of the spot with the vertical and horizontal oscilloscope deflection circuits. A lens focuses the lissajous figure at a plane where various apertures of different geometry can be placed. Beyond the aperture a photomultiplier detects the light passing through the aperture. The output of the photomultiplier is then processed and the position signals are obtained.

The validity of the simulation was verified by comparing the simulation results obtained with a circular aperture and circular scan pattern with results obtained with an actual tube which had a circular aperture and used a circular scan. In each case, the aperture diameter was the same as that of the lissajous figure. The results are shown in figures 3 and 4. In figure 3, which was obtained from the simulation, the abscissa is the ratio of image displacement on the reticle to reticle size. (All subsequent data from the simulation were plotted in this manner.) The basic shape of the curves of figures 3 and 4 is identical and there is no serious departure between the two.

SIMULATOR INVESTIGATIONS OF APERTURE AND SCAN COMBINATIONS

Apertures Utilizing a Circular Scan

Initial investigations utilized a circular reticle and scan pattern as shown in sketch (a1). The length l is the portion of the scan pattern which passes through the reticle. As is shown, the reticle and scan pattern had the same diameter. Sketch (a2) shows the variation of l with ϵ. The transition from $-\epsilon$ to $+\epsilon$ at null will be detected as a change from positive to negative error signal when phase demodulated against the sweep signal. The derived error characteristic will then be of the form shown in sketch (a3). Note that this error signal is a discontinous function and hence has no linear region but rather a step at null.

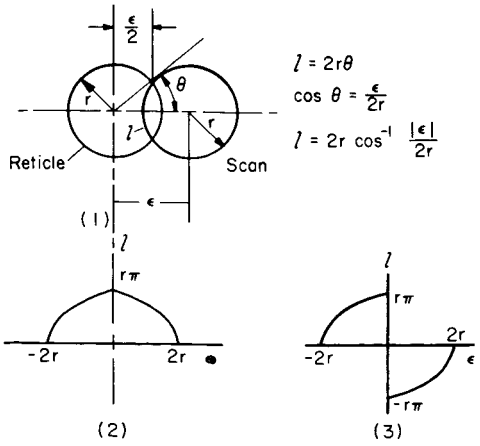

Sketch (a)

Actually, the finite diameter of the star image on the photocathode will result in a small linear region as shown in figure 3, which is a plot of laboratory data obtained with the simulation apparatus. Figure 4 is a plot of a similar error characteristic obtained with an actual FW-129 image dissector tube. As has already been noted, this curve verified the authenticity of the simulation procedure and illustrated the undesirably small linear range and high cross coupling of

the basic tube. From an inspection of the aperture and scan combination it can be seen that there is no star presence signal at null.

From a consideration of the circular aperture with the circular lissajous figure, two distinct types of reticles evolved. With these, an extended linear region as well as a signal indicating null can be obtained by interrupting the electron image beam as it is scanned around the aperture. The two types of reticles are shown in sketch (b).

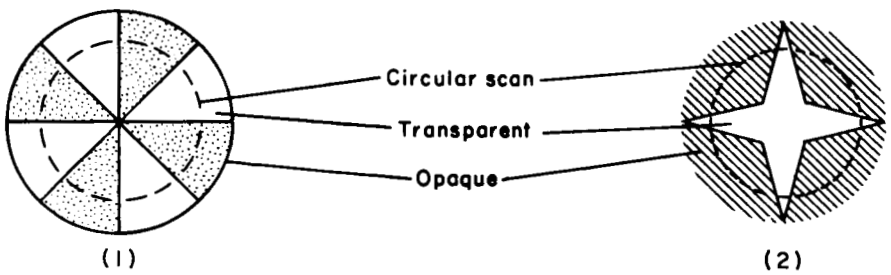

Sketch (b)

In sketch (b1) the centroid of each transmitting sector is near the periphery of the reticle. For a given displacement, the amount of energy transmitted through the reticle is greater on that side of the circular scan farthest from the reticle center as long as the scan lines lie entirely within the reticle area. When the scan is partially on the reticle, the energy transmitted is larger on the side of the scan nearest the reticle center. Thus, with such a reticle an undesirable 180° phase reversal can occur. In sketch (b2) the reticle has its largest opening at the center so the transmitted signal is always greater on that side of the scan nearest the reticle center. Because of the signal phase reversal characteristics of reticles of the type in sketch (b1), the laboratory investigation was confined to the type shown in sketch (b2). Generally, it appears that whenever a position signal is to be determined according to pulse position using a circular scan, the aperture should have its largest opening at the center or null position. The characteristics of a star reticle with twice as many points, as shown in sketch (b2), are shown in figures 5 and 6. Note that the linear range has been extended appreciably compared to figure 3. A null indication signal can be obtained from this aperture by noting that a continuous series of pulses uniformly spaced in time will exist at null.

Double Line Scan

A two-axis error characteristic with an improved linear region can be achieved if a double line scan is used with an aperture with a sinusoidal contour, as shown in sketch (c). This type of scan is generated by driving the horizontal deflection coil with a square current waveform and the vertical deflection coil with a sinusoidal current of frequency twice that of the square wave.

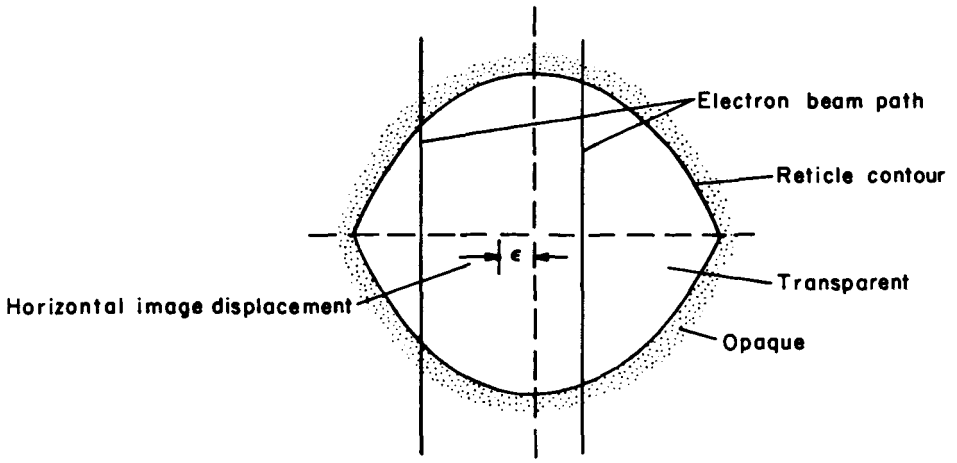

Sketch (c)

Vertical error displacement of the image is determined by the tube output pulse position with respect to the vertical sweep signal; horizontal error displacement is determined by the difference between output pulse width occurring during each vertical sweep. The results of this scan and aperture combination as determined with the simulation apparatus are shown in figures 7 and 8.

Edge Tracking Scan

Optical image position information can be obtained from an image dissector by servoing the electron image to follow either the upper or lower edge of the aperture. Such a system, called edge tracking, operates in the following manner. A triangular sweep signal drives the horizontal deflection coil, and the vertical deflection coil is driven by the output of the tube. Thus, when the electron image is incident on the aperture, a tube output signal will drive the image to the edge of the aperture. The output signal, of course, disappears as soon as the image fails to pass through the aperture. The result is that the image stops on the edge with a sufficient portion of the electron beam passing through to maintain a vertical deflection signal to keep the image on the edge. The current through the vertical deflection coil is then proportional to the displacement of the image on the photocathode in the vertical direction. Horizontal position information is obtained when the phase of the output signal is measured with respect to the scan signal. The simulator investigation utilized a circular aperture and a triangular wave form for the horizontal scan. Vertical polarity information was obtained by tracking both edges of the aperture on alternate half cycles of the horizontal deflection signal. The results obtained from the simulation are shown in figures 9 and 10. It will be noted that a substantial linear region is present.

Saw-Toothed Aperture

From three types of scan patterns and reticle combinations considered in the preceding sections, a combination was simulated that would be particularly compatible with spacecraft mission requirements. The system, synthesized,

employs a saw-toothed aperture (fig. 11) and provides two-axis position information. It employs a simple, single horizontal line scan pattern that involves a minimum of electronic circuit complexity.

The use of a single horizontal axis deflection signal requires a reticle contour that is unsymmetrical about its horizontal axis in order to determine the vertical direction of image displacement. The saw-toothed design in figure 11 satisfies this condition. To understand the operation of this reticle, first consider vertical image displacements. As the electron image is deflected across the triangular-shaped openings by the horizontal scan, a series of pulses will appear across the anode load resistor. The pulse frequency is the intelligence that indicates the vertical direction of the image displacement. For this reason, the number of openings in the reticle is greater below the null axis than above. For image displacement further away from the null axis, the width of each pulse increases, though the spacing and number of pulses remain the same. A Fourier analysis (appendix B) of the pulse train shows that a harmonic of the scan frequency related to the number of triangular-shaped openings is present, which increases in amplitude with the pulse width. The output signal from the tube is fed to separate narrow-band filters which are tuned to frequencies corresponding to the upper and lower sections of the reticle. The difference in the filter outputs is then proportional to vertical image displacement. At null, four pulses indicate star presence; the small diamond-shaped openings on the reticle are for this purpose and also to provide horizontal information at vertical null. Image displacement in the horizontal direction is determined by the position of the pulse train with respect to the sweep signal. This characteristic is derived by filtering the fundamental or sweep frequency from the tube output and phase demodulating this with respect to the sweep signal.

The two-axis error characteristics derived by placing the saw-toothed reticle in the simulation apparatus are shown in figures 12, 13, and 14. The error signals in both the horizontal and vertical axes have a substantially larger linear region than that obtained with any of the previous schemes. Also, the cross coupling is less than that for the previous schemes. A star presence signal at null is provided and the electronic sweep circuitry is very simple. Thus all four of the criteria set forth for an improved star tracker are satisfied to a high degree. Although all of the reticle shapes previously considered were capable of giving the desired characteristics to some degree, the saw-toothed reticle appeared to best fulfill the aims of this investigation. A saw-toothed reticle was therefore chosen to be incorporated in an actual tube.

IMAGE DISSECTOR WITH MODIFIED APERTURE

In order to verify the conclusions of the simulator investigations, a saw-toothed reticle was incorporated into an International Telephone and Telegraph tube type FW-129. The FW-129 is an end window, magnetic deflection, electrostatic focus, image dissector tube with an S-11 photocathode surface 1 inch in diameter. Figures 15 through 18 present the results of tests in which the tube is used to determine the feasibility of employing it as a

detector in point source tracking applications. Figure 15 shows the vertical error signal and the signal cross coupled into the horizontal channel for a vertical displacement of a 1-mil-diameter light spot on the photocathode. The total linear region of the vertical characteristic is 0.22 inch on the photocathode, which is 22 percent of its diameter. The cross coupling into the horizontal channel is 1 percent. When these results are compared with results obtained with the unmodified FW-129 with a 0.07-inch-diameter circular aperture (fig. 4), it is observed that the width of the linear region is substantially increased. In figure 4, the total linear region is 0.008 inch displacement on the photocathode, which corresponds to 0.8 percent of the photocathode diameter.

Figures 16 through 18 show the characteristics of the tube for a horizontal displacement of a 1-mil light spot on the photocathode. Figures 16 and 17 show the horizontal characteristics for the high and low frequency sides of vertical null. These curves have the same slope, but one is slightly wider than the other because of the difference in reticle width. The total linear region of these characteristics corresponds to 0.17 inch on the photocathode or 17 percent of its diameter. Figure 18 shows the error characteristic of the tube at vertical null for a displacement in the horizontal direction. It will be observed that this characteristic is less in magnitude than the other two horizontal characteristics. This condition is due to the decrease in width of the triangular sector as the null point is approached.

The error characteristics for the modified FW-129 exhibit a substantial linear region and a cross coupling that is quite small. This indicates that the tube could be effectively used in tracking applications.

Photometric tests of the tube showed that it had the same luminous sensitivity as the standard tube but higher dark current versus dynode supply voltage characteristic. The dark current at 1700 volts dynode supply for the standard FW-129 (circular aperture 0.07-inch diameter) is 0.01 microampere, while for the modified tube the dark current is 0.1 microampere. The dark current characteristics for the modified tube are shown in figure 19. The reason for the increased dark current is believed to be the increased reticle aperture size (0.3-inch width and 0.25-inch height) and the correspondingly increased effective cathode area.

A Two Reticle System

From the study undertaken, the idea of putting a reticle on the photocathode to obtain a true null became apparent for reasons to be discussed. An inherent problem of the image dissector tube is that its deflection system is susceptible to local electrostatic and magnetic fields, which could upset the electrical null position. A common method of avoiding this effect is to use shielding. Another method of overcoming this problem might be by the addition of a second reticle placed on the photocathode. When considering the origin from which position information is to be derived, two zeros must be taken into account, the optical and electrical. The optical zero is fixed by the optics of the system. The electrical zero is determined by the electronic beam position at optical zero and with no current through the deflection coils; but

it is subject to external fields when not properly shielded. It should be possible to place a reticle on the photocathode to code a pattern on the electron beam. By comparing this with the reticle at the electron image plane it should be possible to detect the optical zero in the presence of a disturbing field. Such an arrangement might also be utilized to determine the magnitude of the field.

CONCLUSIONS

The internal workings of an image dissector were simulated and various combinations of aperture and scan pattern were investigated. Among all other combinations of aperture geometry and scan pattern considered, the combination of a saw-tooth-shaped aperture and straight line scan was found to best satisfy the characteristics desired. The saw-toothed aperture was built in an actual tube and performed as expected. From a comparison of its signal characteristics with that of a circular aperture and circular scan the saw-toothed aperture and single line scan showed a marked improvement in linearity with little cross coupling. Not all conceivable combinations of aperture geometry and scan pattern were examined; however, it can be stated that from these studies it was found that the aperture of the image dissector can be effectively altered to include much of the complexity required in generating position signals and to provide desired signal characteristics.

Ames Research Center
National Aeronautics and Space Administration
Moffett Field, Calif., June 17, 1965

APPENDIX A

DISCUSSION OF IMAGE DISSECTOR TUBE OPERATION

The image dissector is a photoelectric tube which has the capability of examining an optical image electronically. The major parts of the tube are the photocathode, deflection section, electron image plane, and the electron multiplication section (see fig. 20). In operation, an optical image on the photocathode causes electrons to be emitted from the photoemissive inner surface of the photocathode. The distribution of electrons is directly proportional to the light energy incident on the photocathode. The electron image is defined as the electron distribution in a two-dimensional plane corresponding to the distribution of light energy of the optical image. This electron image is accelerated to the electron image plane where it comes to a focus. In the absence of a magnetic or electrostatic field, the position of the electron image relative to the tube axis is the same as that for the optical image. Placed at the electron image plane is an aperture which leads to the electron multiplication section of the tube. Only those electrons that enter this aperture result in a tube output. With a suitable deflection system, it is possible to scan the electron image across the aperture so that an amplitude versus time signal can be derived corresponding to each point on the image.

In the text of this report a point source (star image) is considered for deriving position information. Figure 2 shows the equipment used to simulate the internal workings of an image dissector for a point source image. The deflected electron image is simulated by deflecting the spot on an oscilloscope. The lissajous figure formed by the vertical and horizontal deflection signals can be moved by the oscilloscope position controls to simulate the displacement of the optical image. Situated a small distance away from the oscilloscope is a lens which focuses the oscilloscope display onto a reticle plate (electron image plane). Light passing through the reticle is collected by a photomultiplier (electron multiplication section). All reticle shapes considered were tested on this simulation equipment.

APPENDIX B

ANALYSIS OF THE OUTPUT OF AN IMAGE DISSECTOR TUBE MODIFIED WITH A SAW-TOOTHED RETICLE

Displacement signals are derived from the saw-toothed reticle in conjunction with a linear saw-toothed deflection waveform. In sketches (d1) and (d2) are shown the output pulse trains for an image displaced above and below the horizontal axis, respectively. A Fourier analysis of these waveforms shows what parameters the horizontal and vertical error signals depend upon.

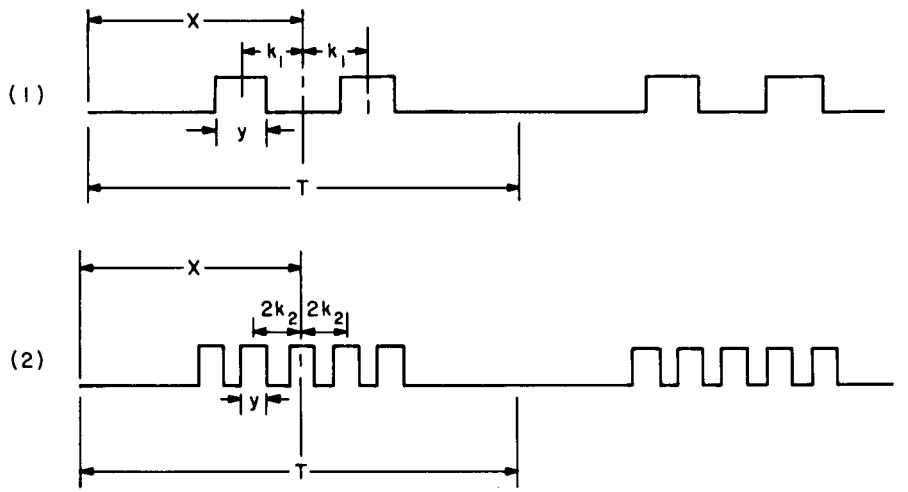

Sketch (d)

T period

X time for start of sweep to midpoint between pulses; varies directly as the image horizontal displacement

y time duration of pulse; varies directly as the image vertical displace-displacement

2k time between pulses

The above waveforms can be written in the following form:

$$E = A_o + \sum_{n=1}^{\infty} A_n \sin n\omega t + \sum_{n=1}^{\infty} B_n \cos n\omega t$$

The horizontal error signal is proportional to $(T/2) - x$ and is determined from the fundamental component of the signal for the two- and five-pulse waveforms by measuring the phase relative to the term $\sin \omega t$. In practice, this involves a phase detector in the horizontal detection circuit.

The fundamental components of signal for the waveforms shown in sketches (d1) and (d2) are:

$$\left.\begin{array}{l}\text{2 pulse}\end{array}\right\} E_1 = \frac{4}{\pi} \cos \omega k_1 \sin \frac{\omega y}{2} \sin \omega(t - x)$$

$$\left.\begin{array}{l}\text{5 pulse}\end{array}\right\} E_1 = \frac{4}{\pi} \left(\cos 4\omega k_2 + \cos 2\omega k_2 + \frac{1}{2}\right) \sin \frac{\omega y}{2} \sin \omega(t - x)$$

It will be noted that the time phase of the two fundamental signals varies directly as the horizontal displacement. It is essential that the rms value of E_1 not be zero in order to generate the horizontal displacement signal. The two parameters k and y could cause the fundamental signal to go to zero; k is a function of pulse separation and can be fixed with the sweep amplitude. Thus the effect of k can be controlled. (For the laboratory investigation, $k_1 = T/8$ and $k_2 = T/20$.) As the vertical displacement, which is proportional to y, approaches zero, the fundamental for both waveforms approaches zero. To keep E_1 from vanishing at the vertical null axis and to generate a star presence signal, small openings are placed on the reticle at the vertical null axis.

The vertical error signal is determined by filtering the fourth and tenth harmonic from the tube output. It can be shown that when an image is above or below the vertical null axis, the fourth or tenth harmonic, respectively, will be present, but not both simultaneously. The magnitude of each harmonic as a function of vertical displacement above and below the axis is the same.

BIBLIOGRAPHY

Atwill, William D.: Star Tracker Uses Electronic Scanning. Electronics, Sept. 1960.

Carpenter, Robert O. B.: Comparison of AM and FM Reticle Systems. Applied Optics, vol. 2, no. 3, Mar. 1963, pp. 229-236, 242.

Getler, Michael: Bendix Star and Planet Tracker Program Locks on New Detector Device. Missiles and Rockets, vol. 13, no. 17, Oct. 1963, pp. 24-25.

Morales, J. J.; and Schenkel, F. W.: Development of a Small Ruggedized Electrostatic Image Dissector. (Paper presented at the Winter General Meeting of IEEE, Jan. 30, 1963.) IEEE Paper CP 63-545.

Sharpe, J.: Photoelectric Cells and Photomultipliers. Electronic Technology, vol. 38, June 1961, pp. 196-201; July 1961, pp. 248-256.

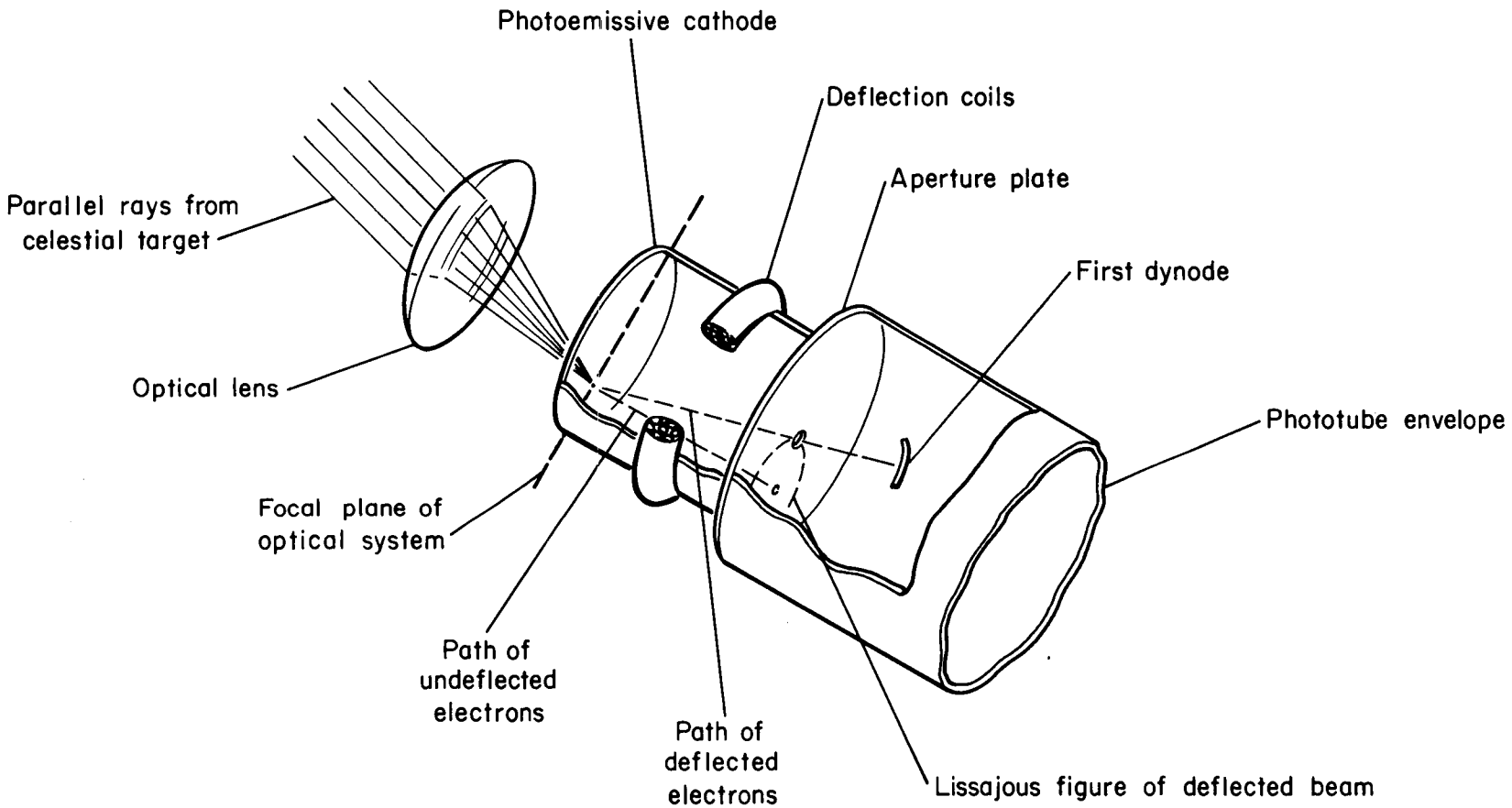

Figure 1.- Image dissector tube as used in a star tracking application.

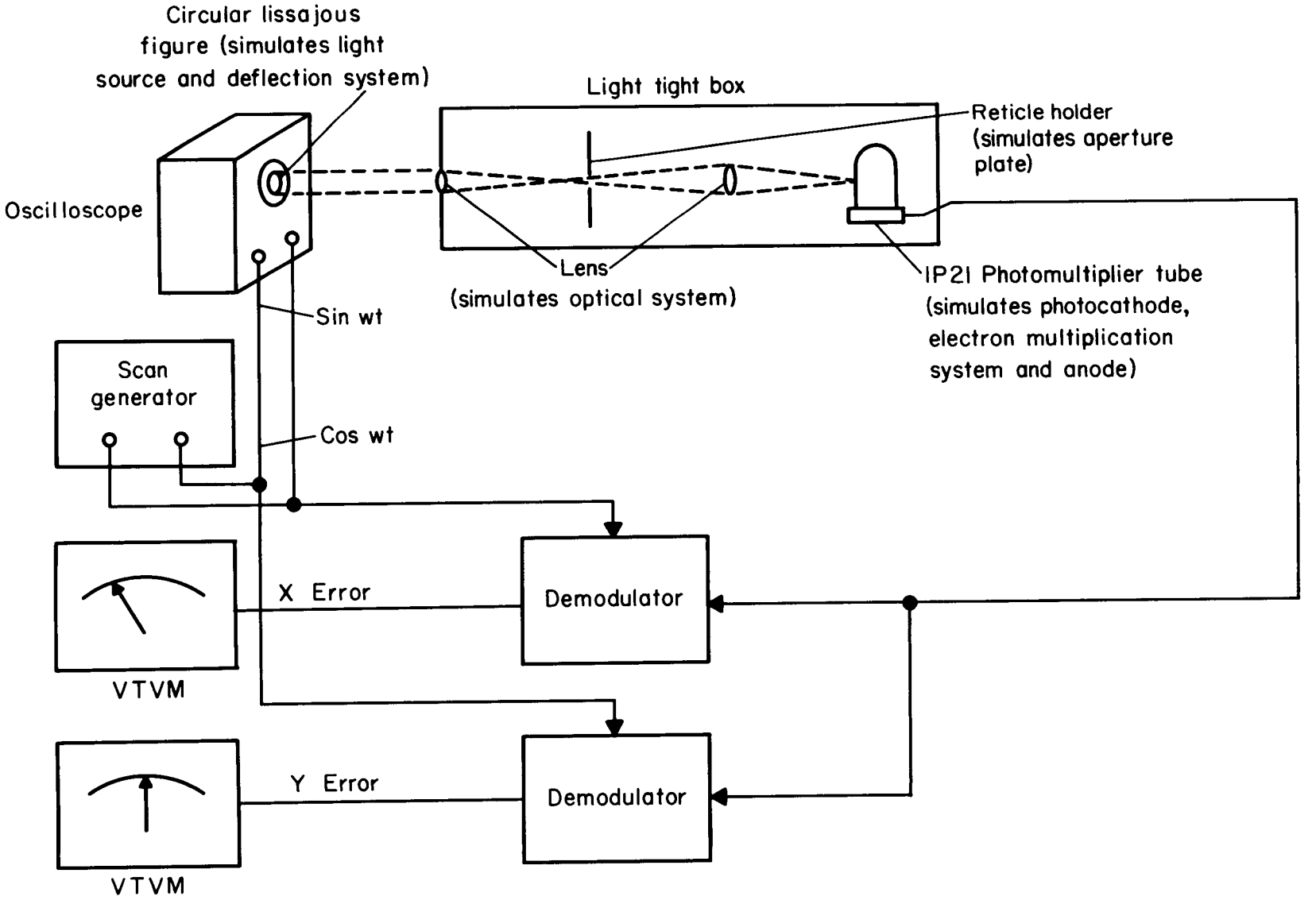

Figure 2.- Laboratory apparatus to simulate the inner workings of an image dissector tube. As shown above, the simulation applies to a circular scan and circular reticle.

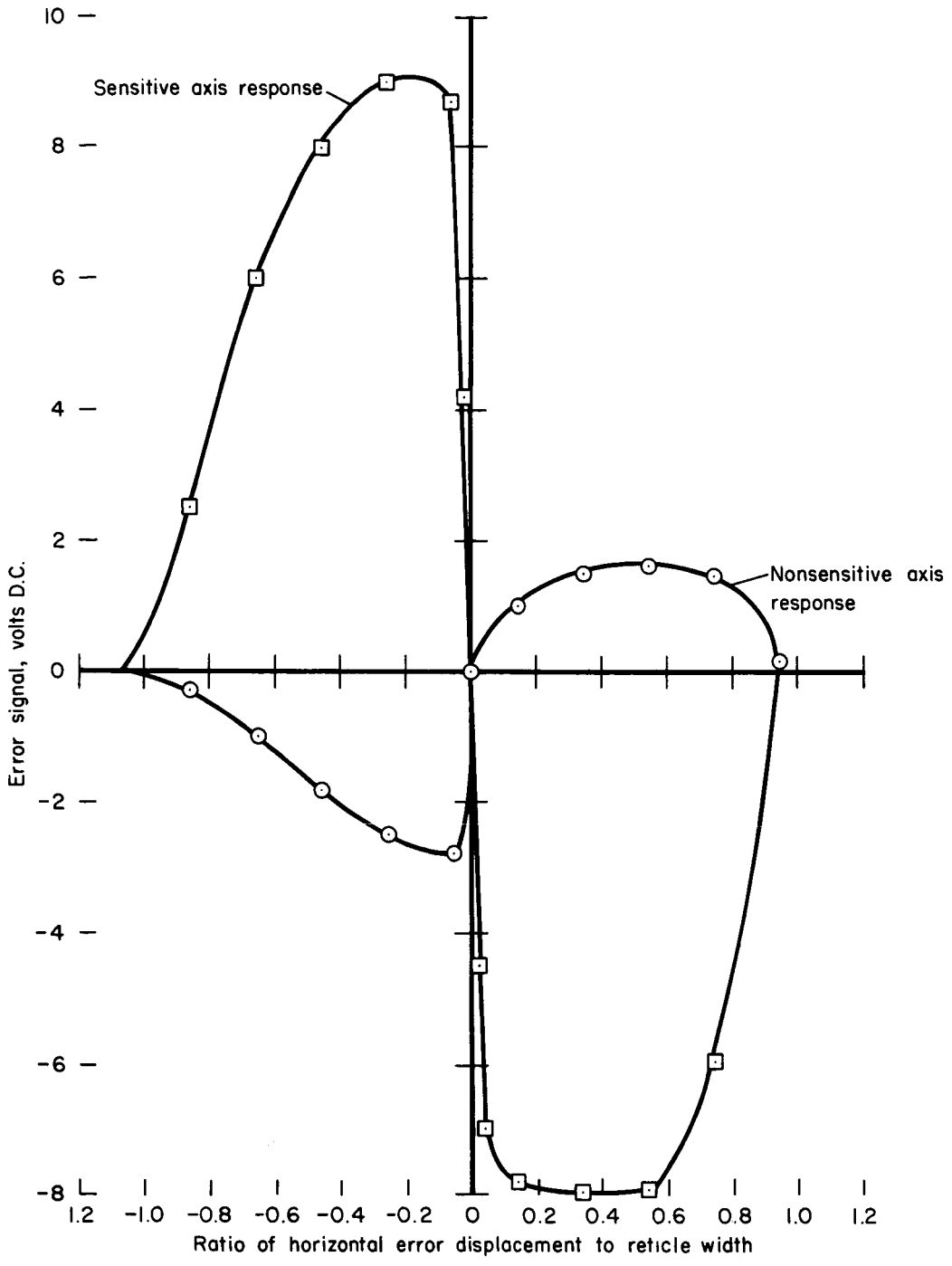

Figure 3.- Laboratory simulation results of the error characteristic for a circular reticle and a circular scan.

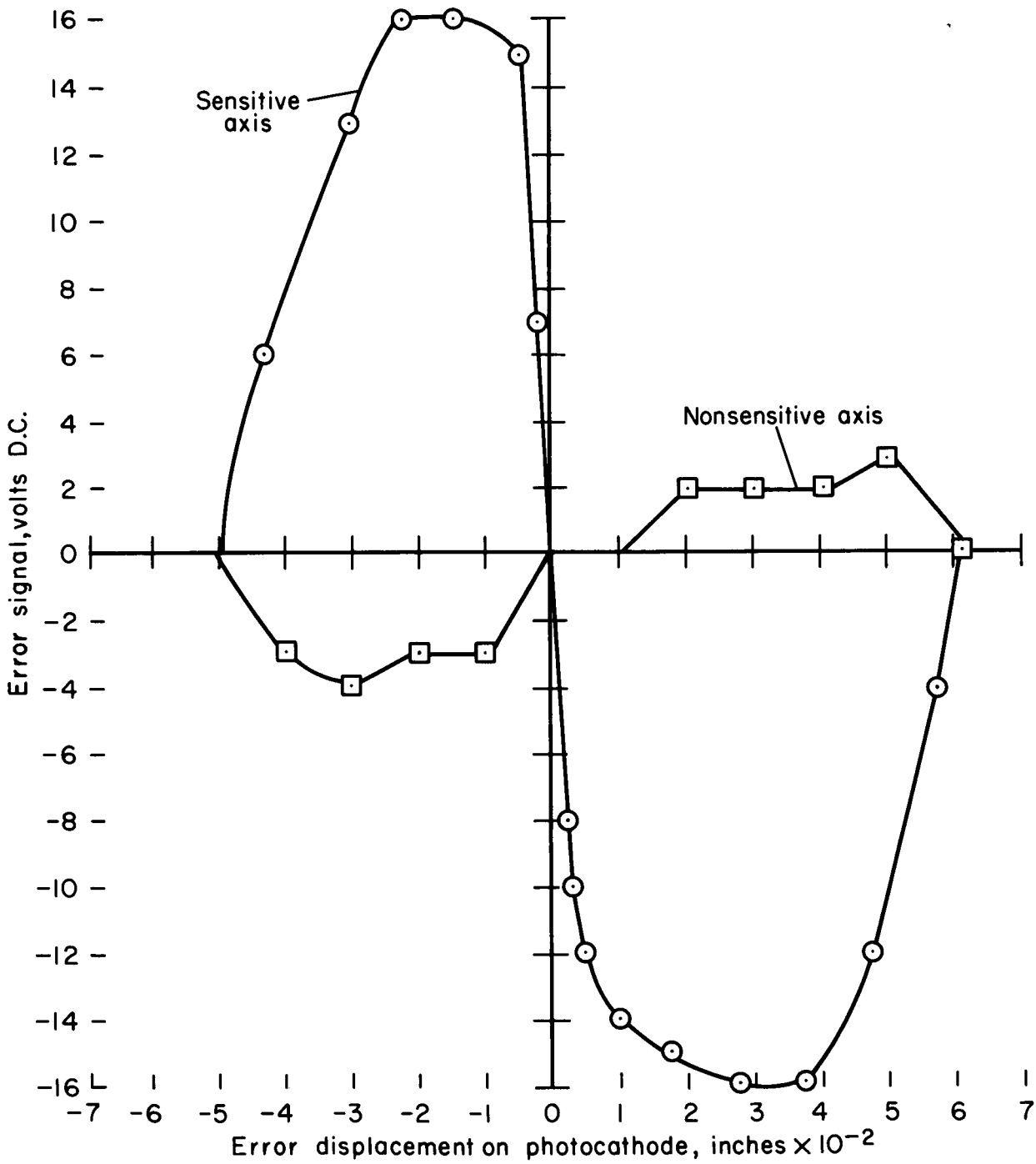

Figure 4.- Error characteristic obtained with an FW-129 image dissector circular aperture (0.07-inch diameter) and circular scan.

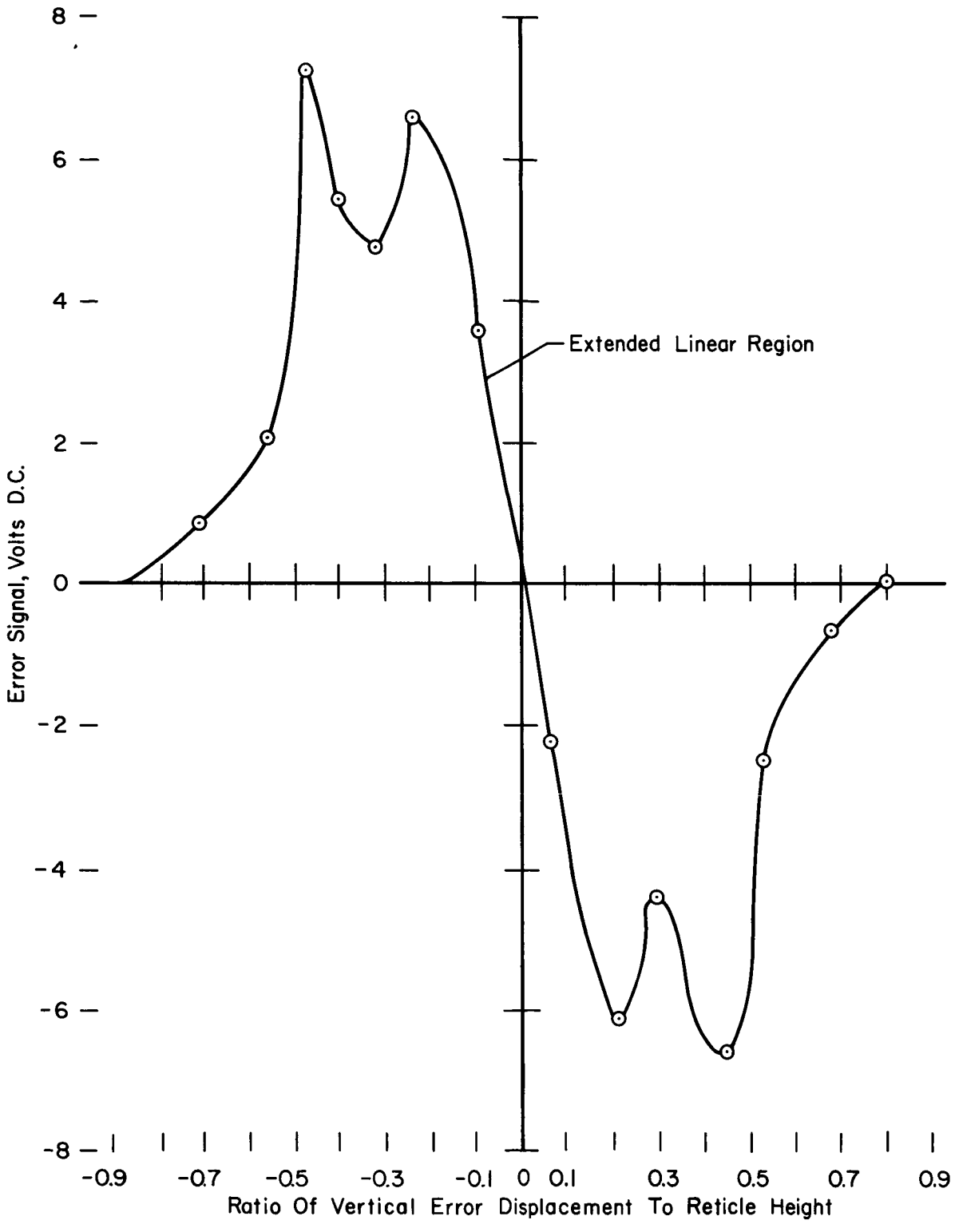

Figure 5.- Laboratory simulation results of the vertical error characteristic obtained with an 8-point star reticle and a circular scan.

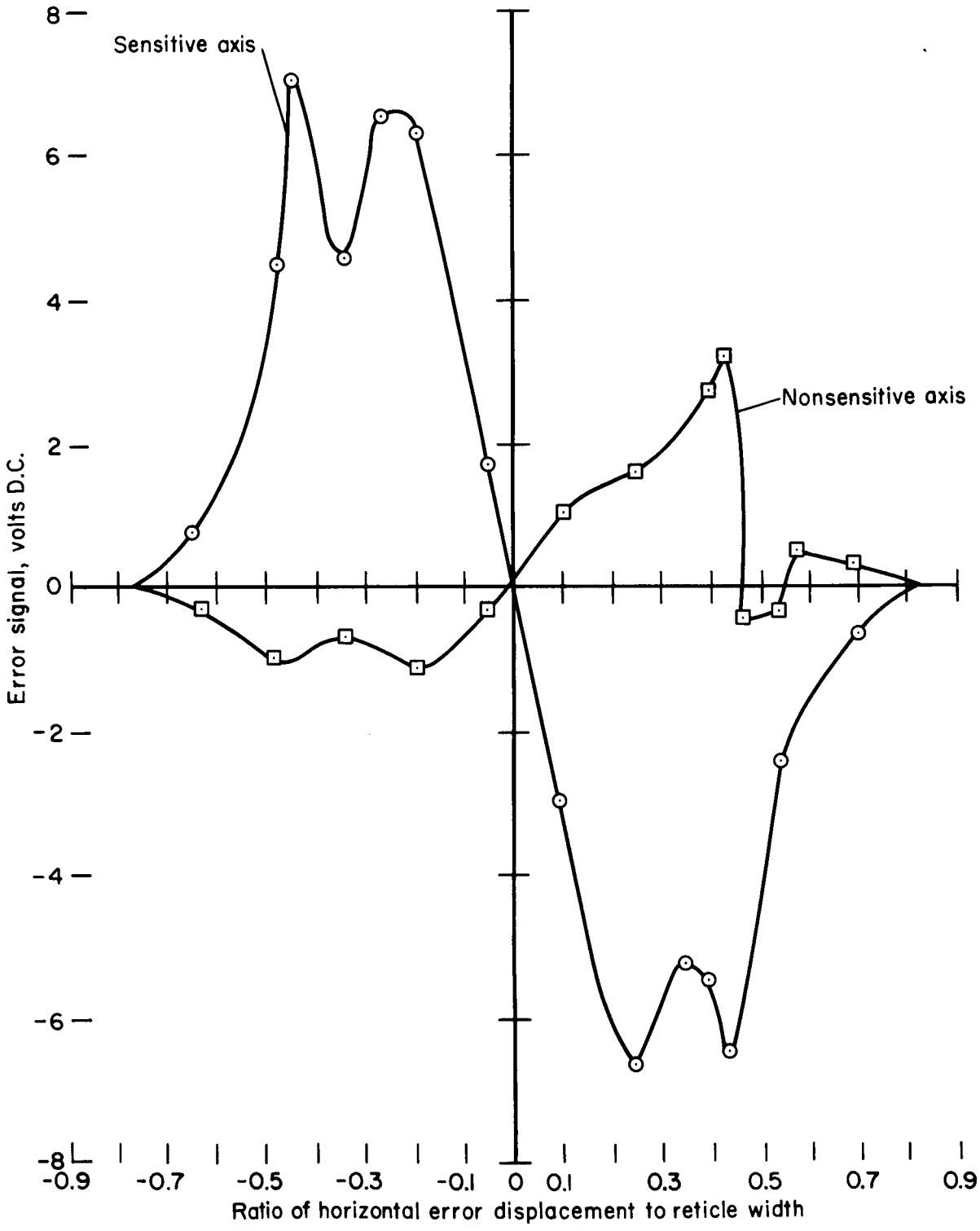

Figure 6.- Laboratory simulation results of the horizontal error characteristic obtained with 8-point star reticle and circular scan.

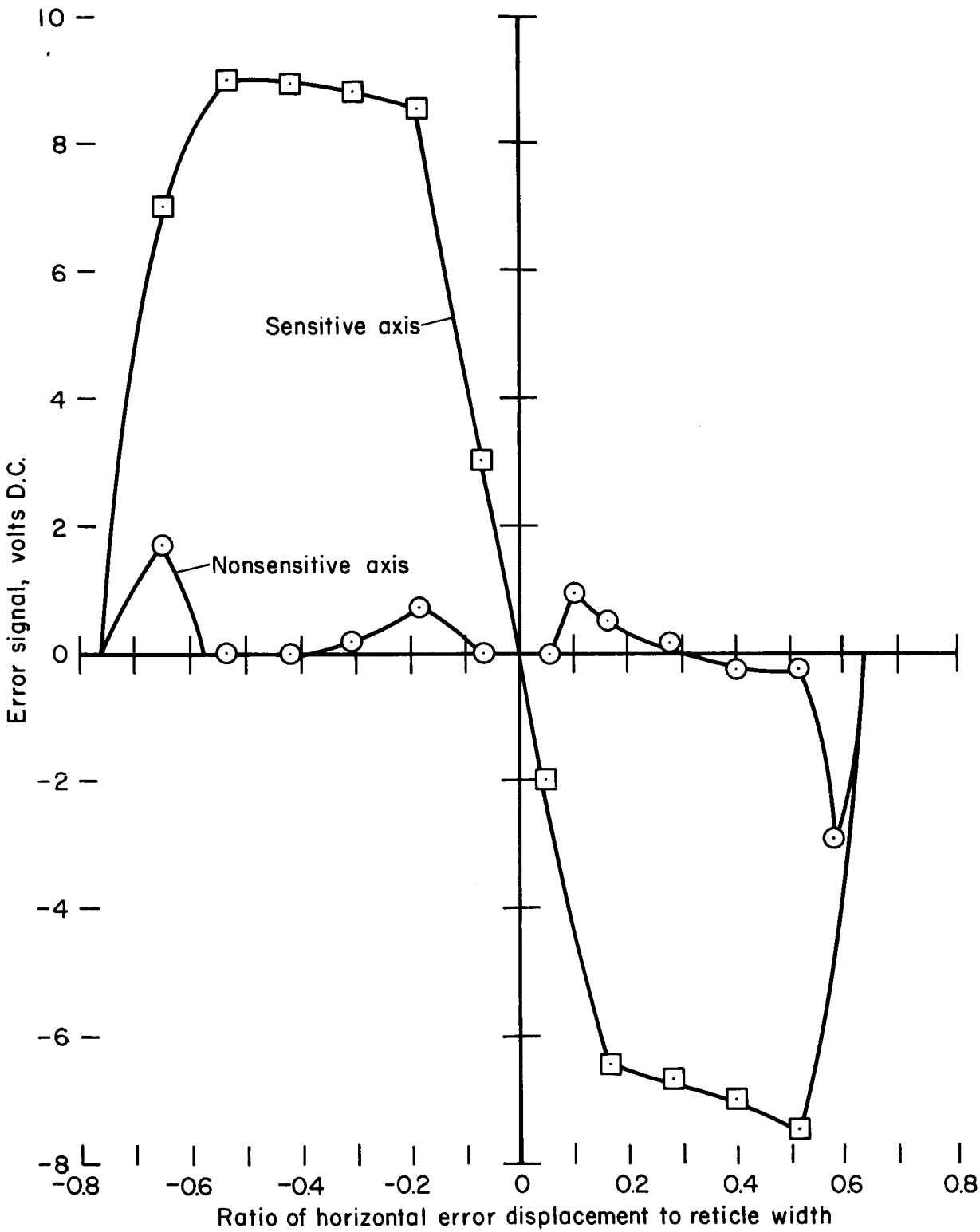

Figure 7.- Laboratory simulation results of the horizontal error characteristic obtained with a sine aperture and a double line scan.

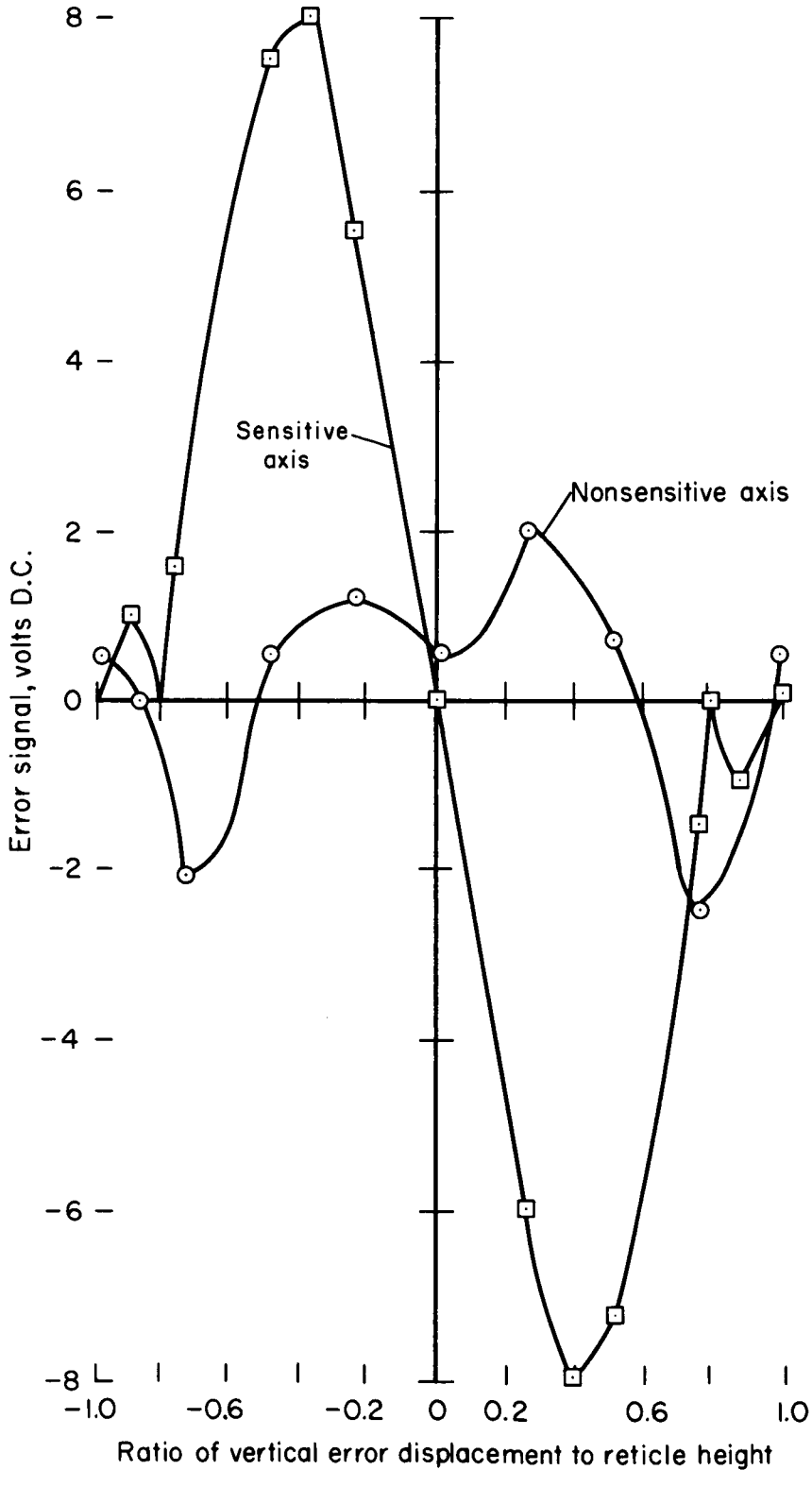

Figure 8.- Laboratory simulation results of the vertical error characteristic with a sine aperture and a double line scan.

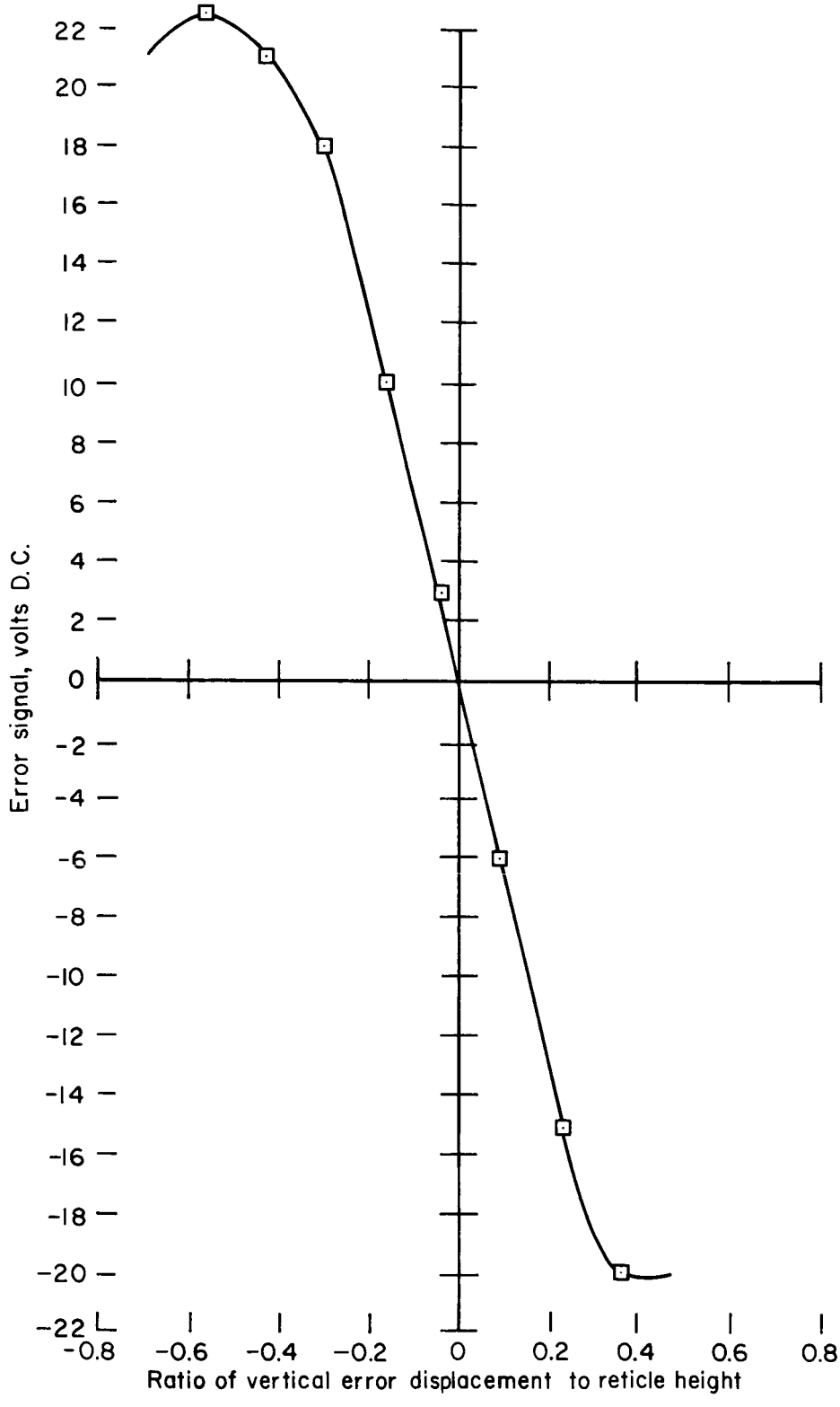

Figure 9.- Laboratory simulation results of the vertical error characteristic obtained by edge tracking a circular reticle.

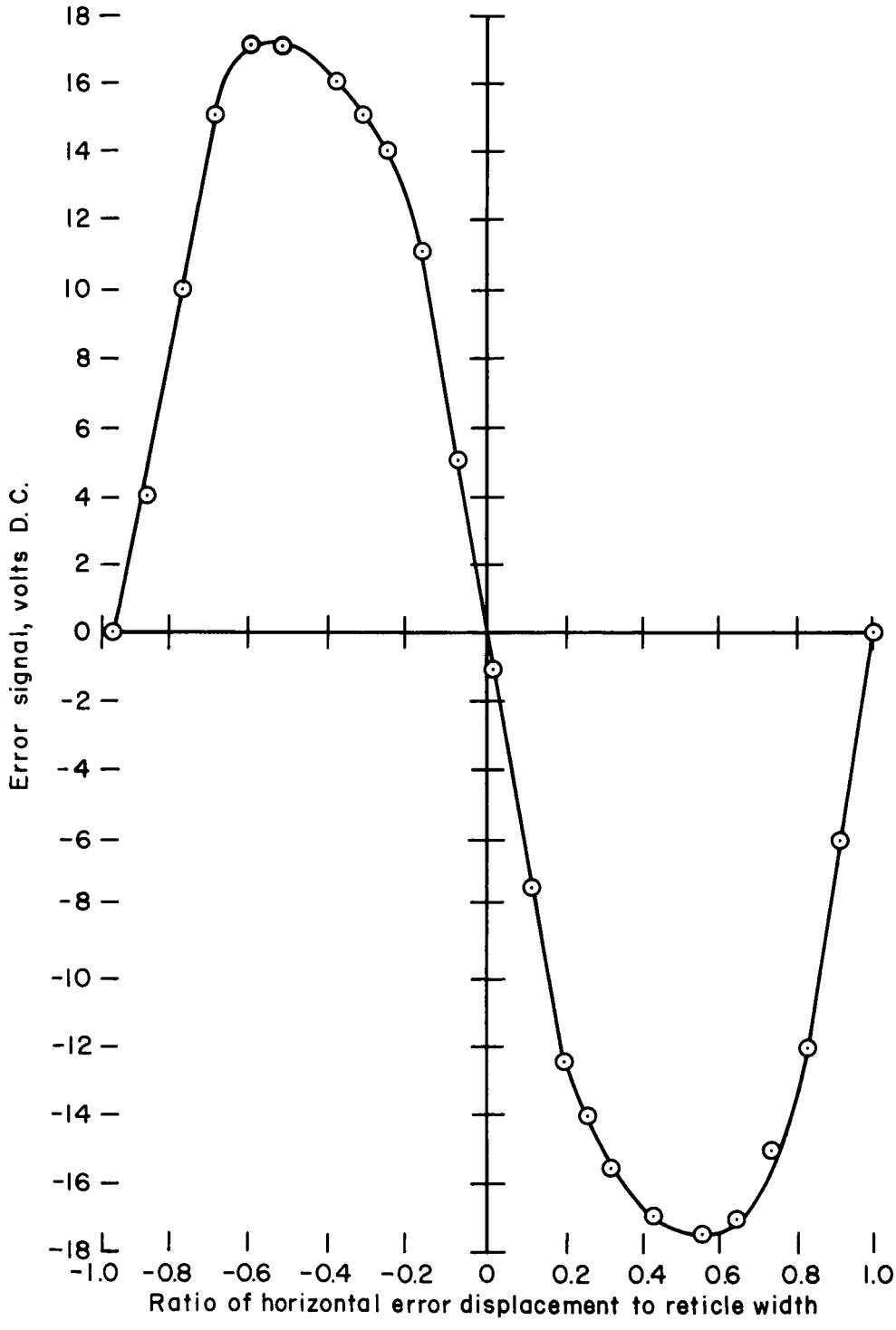

Figure 10.- Laboratory simulation results of the horizontal error characteristic obtained by edge tracking a circular reticle.

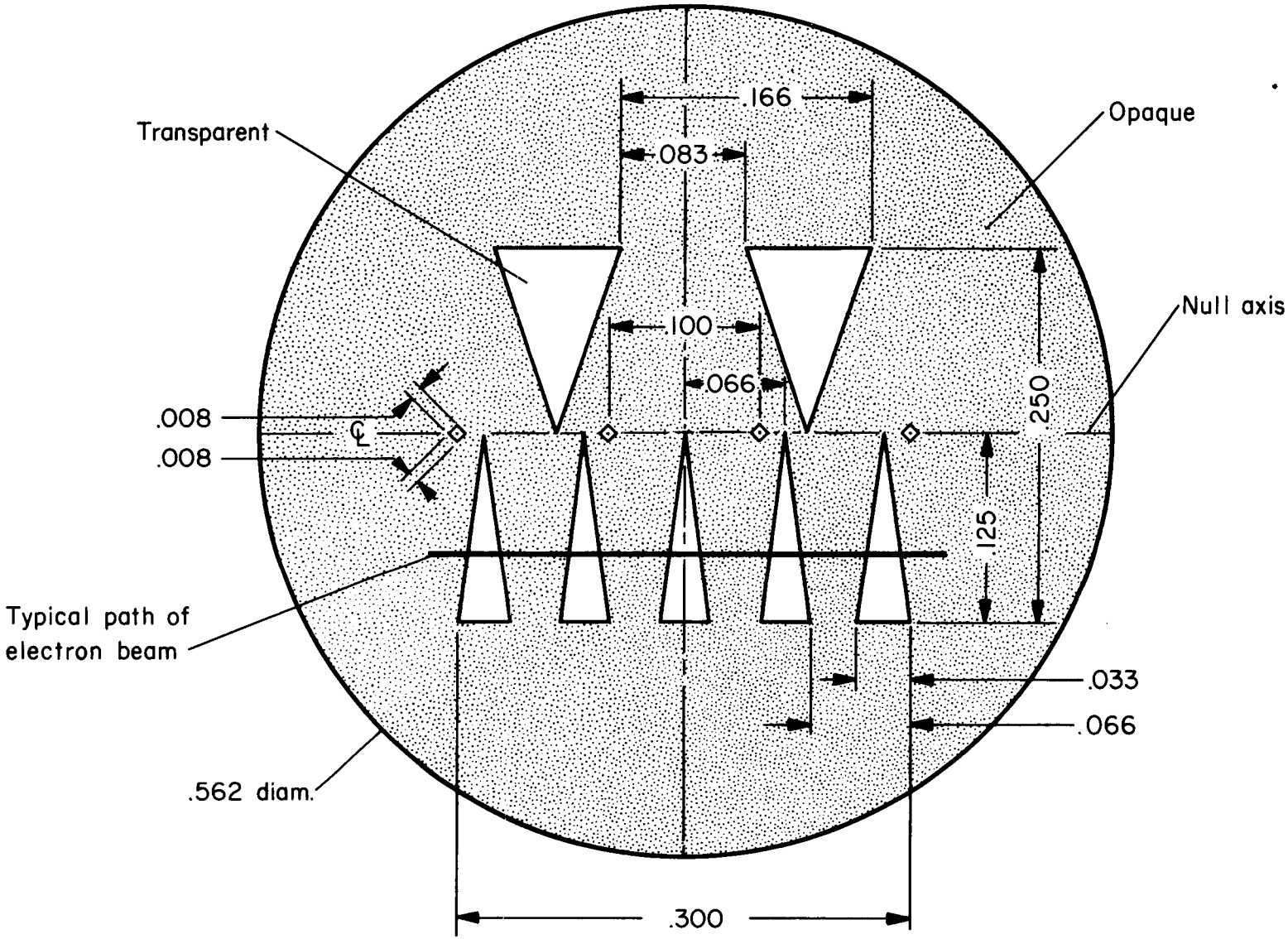

Figure 11.- Saw-toothed-shaped reticle.

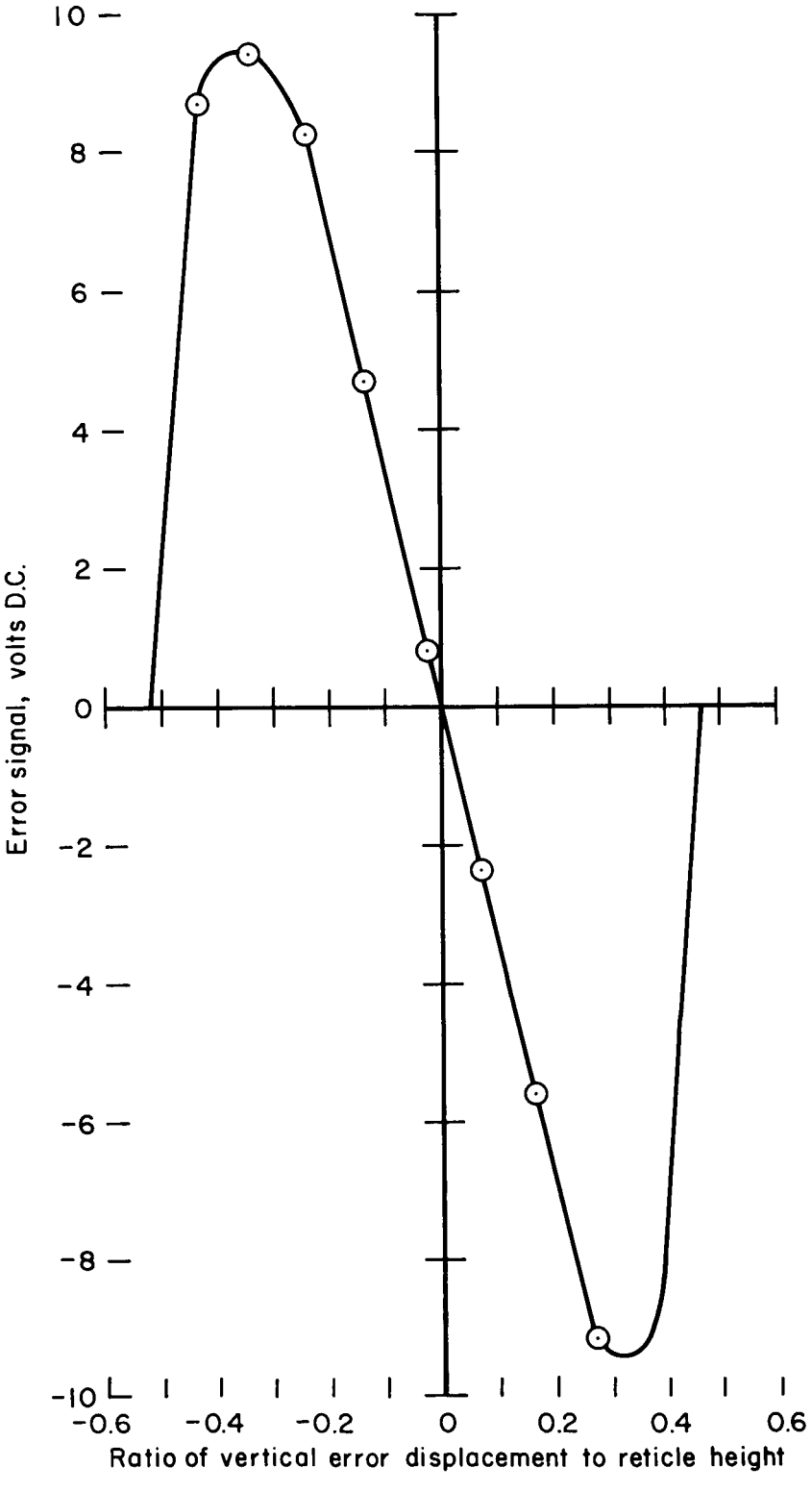

Figure 12.- Laboratory simulation results of the vertical error characteristic with a saw-toothed reticle and a straight line horizontal scan.

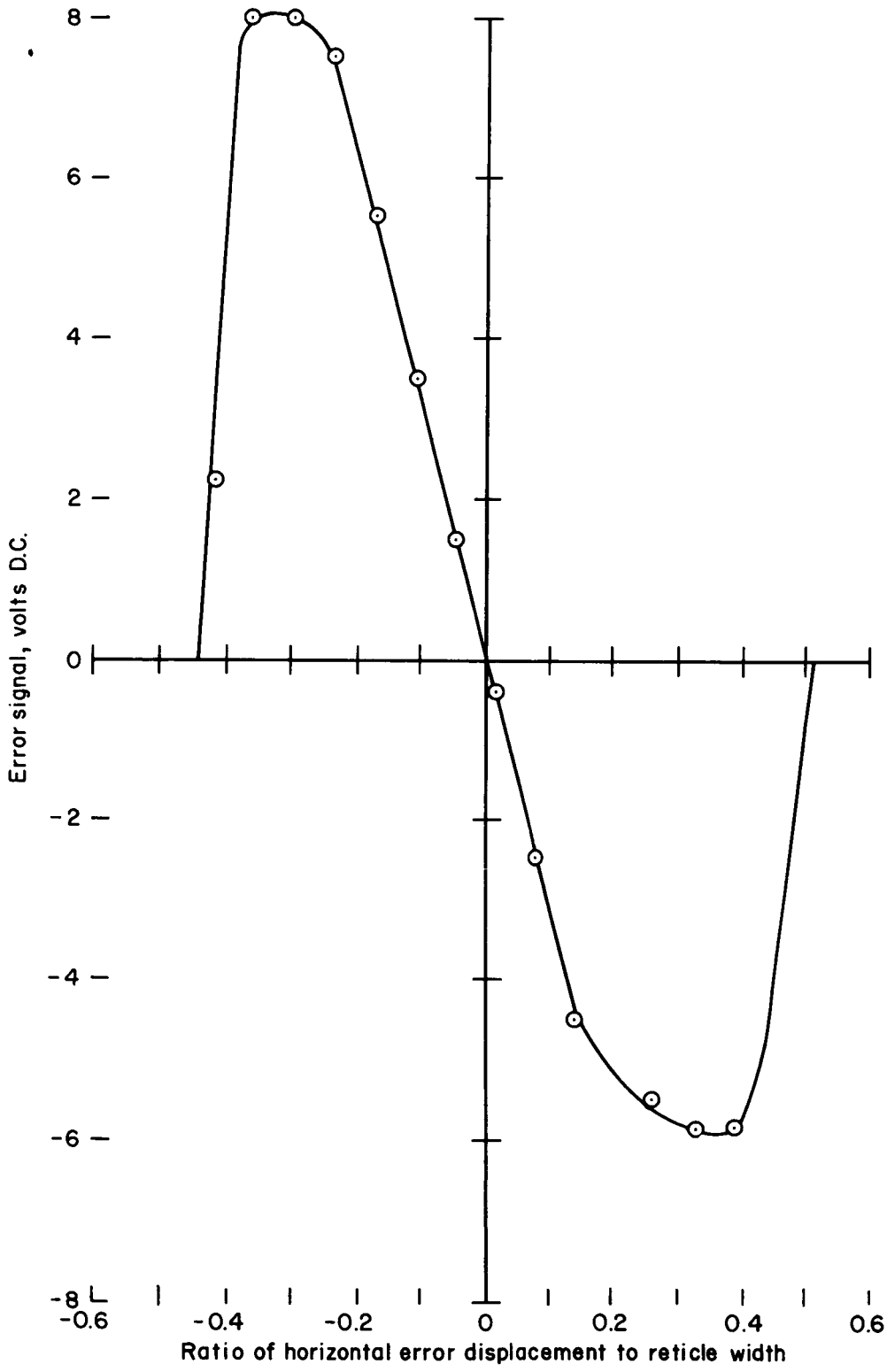

Figure 13.- Laboratory simulation results of the horizontal error characteristic from low frequency side of null with the saw-toothed reticle.

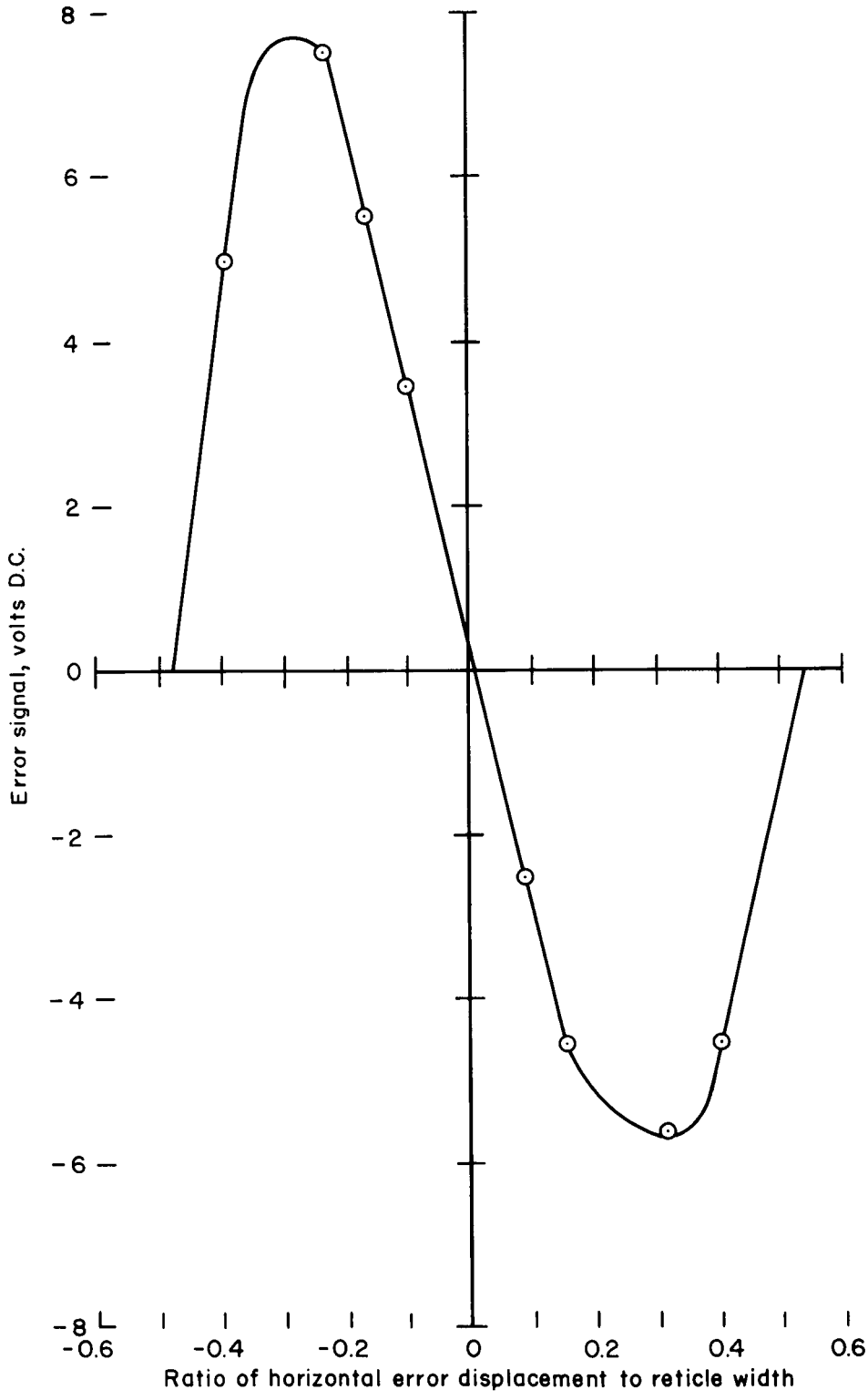

Figure 14.- Laboratory simulation results of the horizontal error characteristic from high frequency side of null with the saw-toothed reticle.

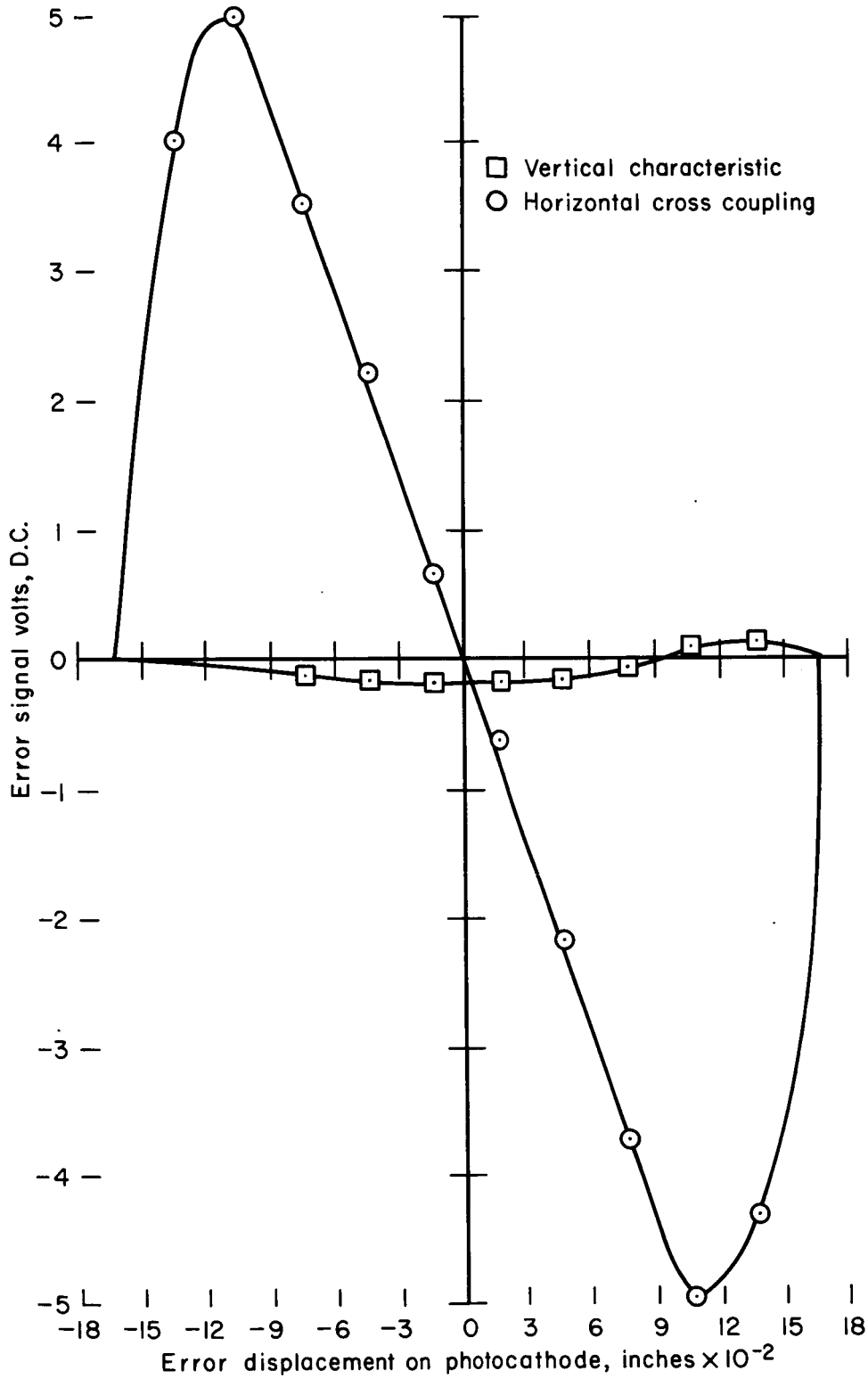

Figure 15.- Vertical error characteristic for modified FW-129 image dissector tube.

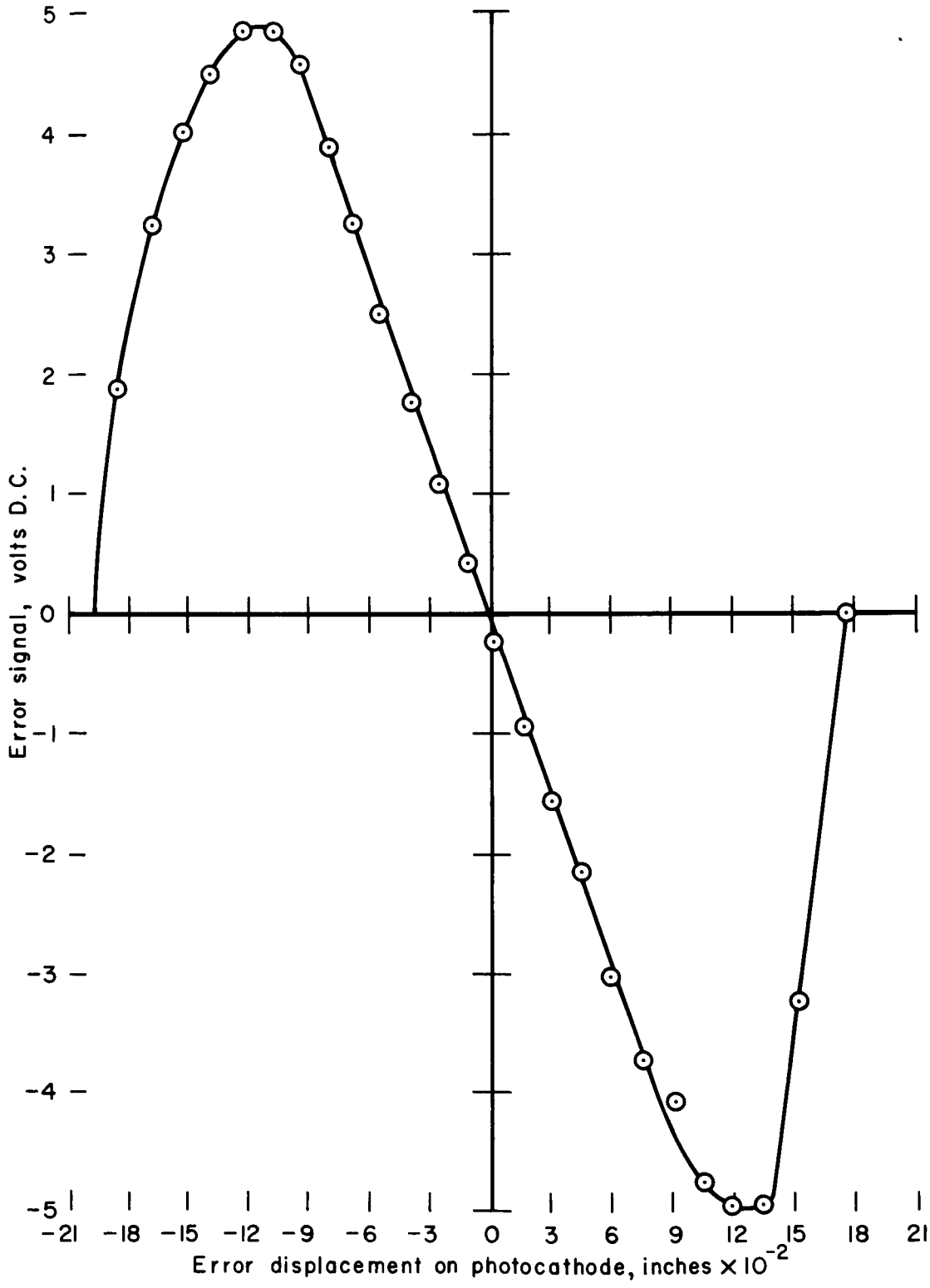

Figure 16.- Horizontal error characteristic from high frequency side of null for modified FW-129 image dissector tube.

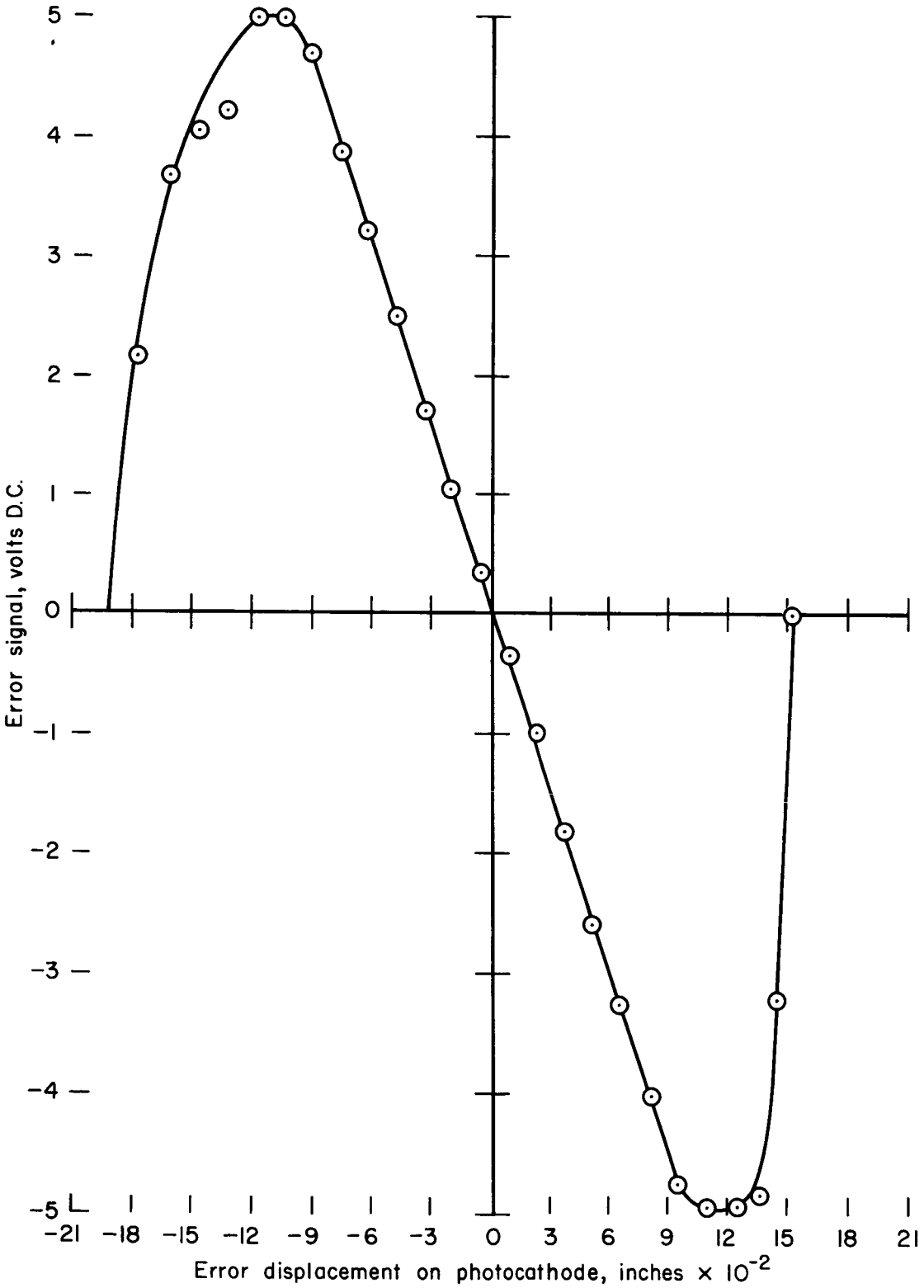

Figure 17.- Horizontal error characteristic from low frequency side of null for modified FW-129 image dissector tube.

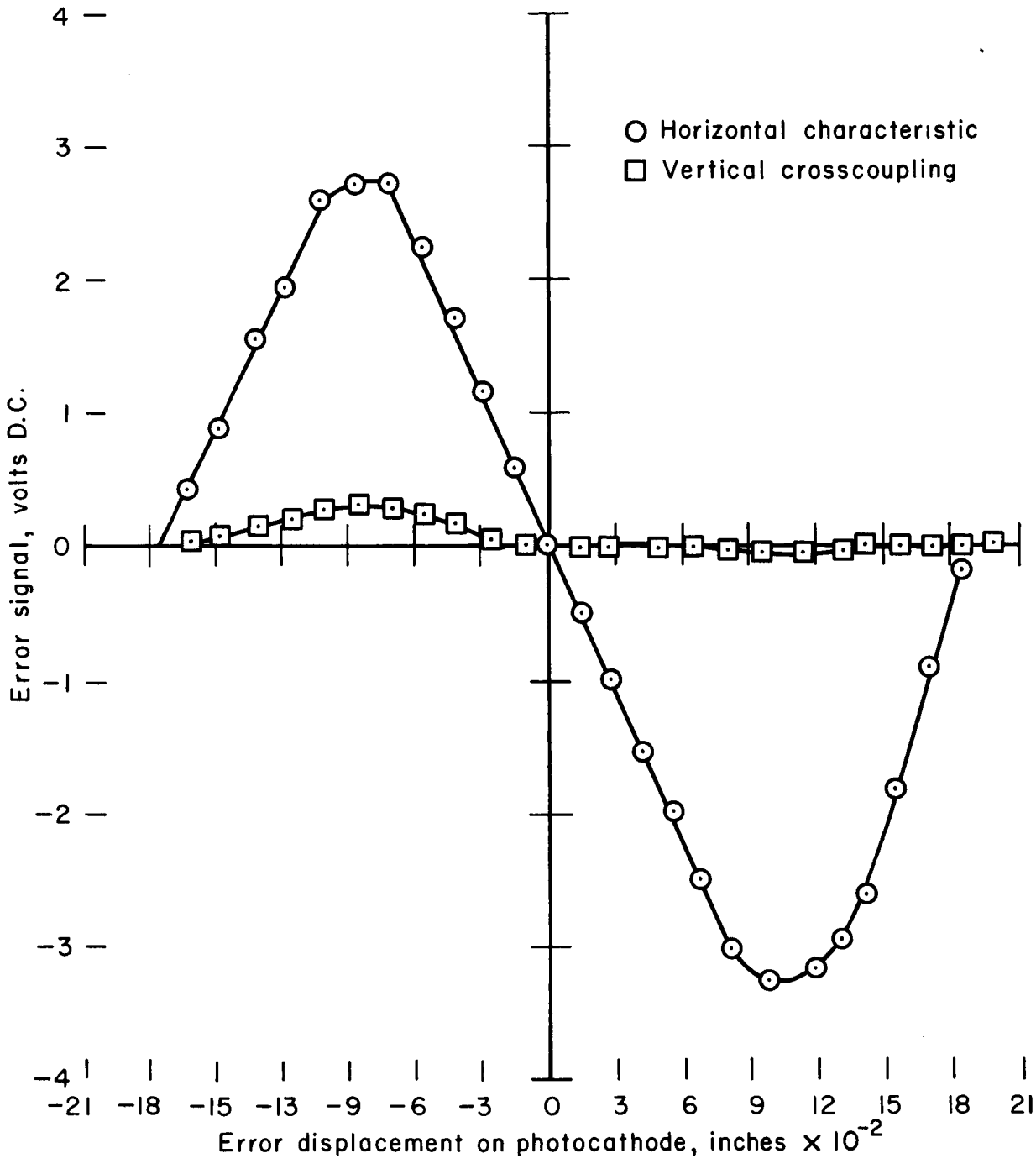

Figure 18.- Horizontal error characteristic at vertical center for modified FW-129 image dissector tube.

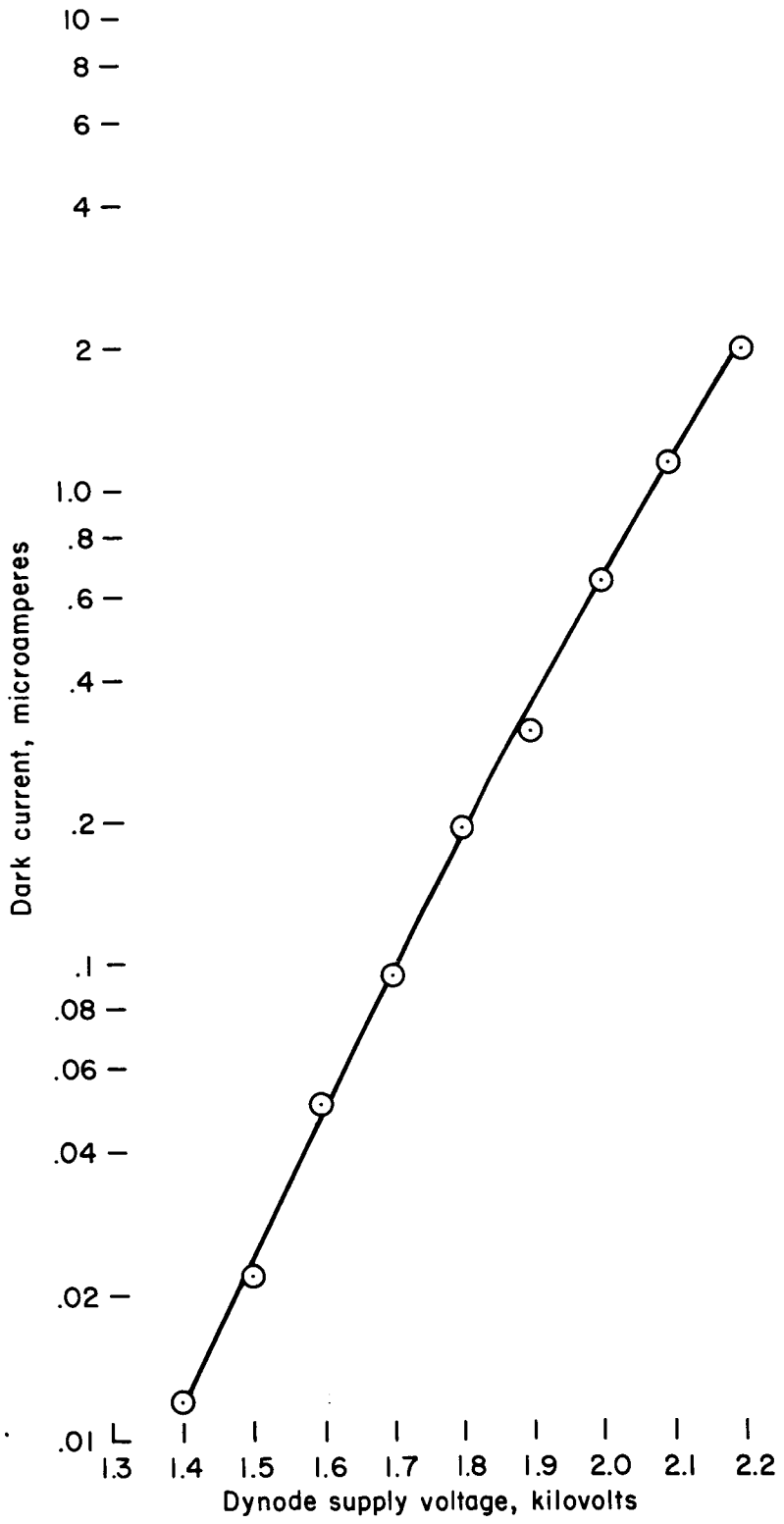

Figure 19.- Dark current characteristic for modified FW-129 image dissector.

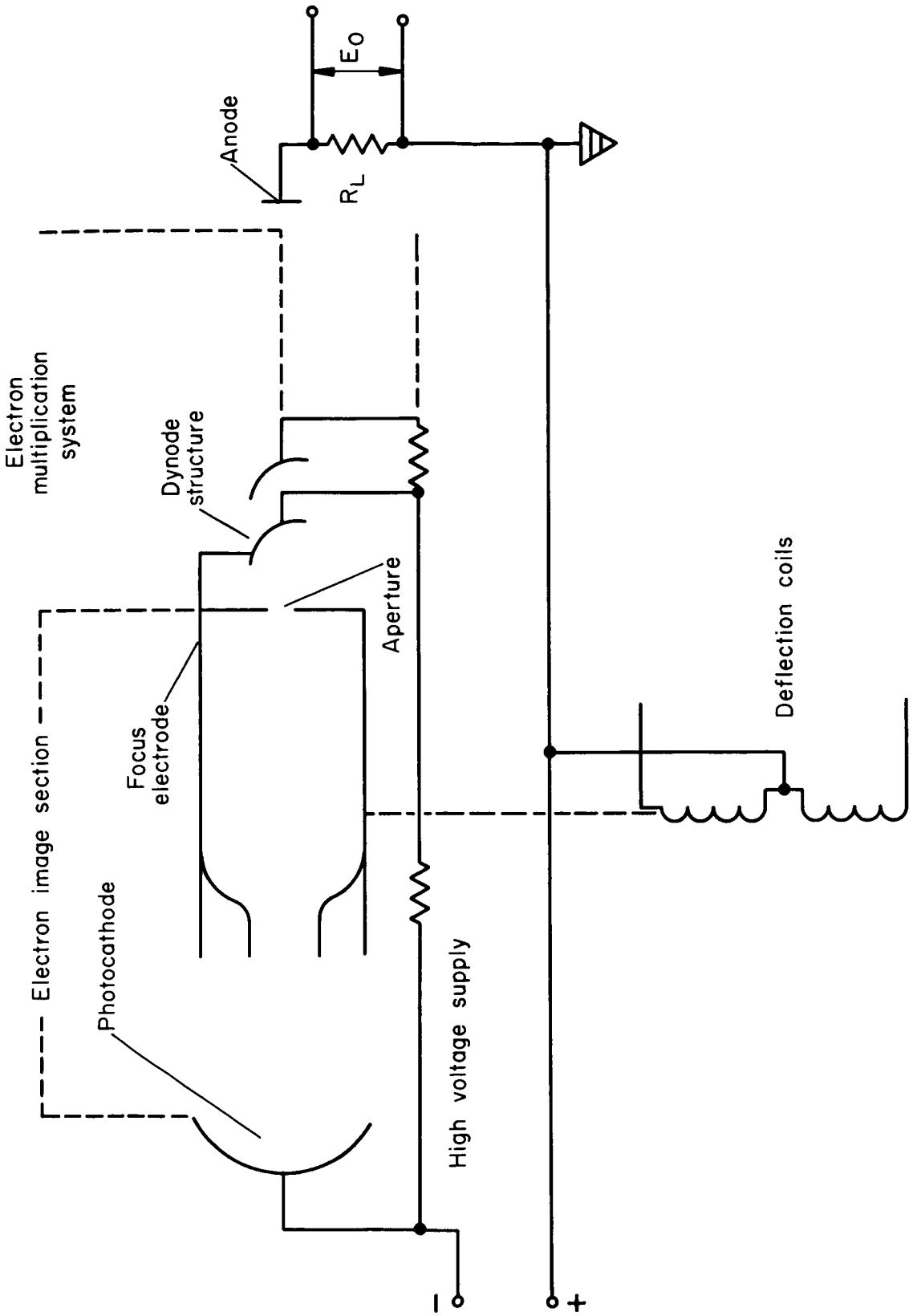

Figure 20.- Image dissector tube.

NASA-Langley, 1965 A-1099